Microprobe techniques for speciation analysis and geochemical characterization of mine environments: The mercury district of Almaden in Spain

ARTICLE *in* ENVIRONMENTAL SCIENCE AND TECHNOLOGY · AUGUST 2006

Impact Factor: 5.33 · DOI: 10.1021/es052392l · Source: PubMed

6 AUTHORS, INCLUDING:

Xavier Gaona
Karlsruhe Institute of Technology
41 PUBLICATIONS **300** CITATIONS
SEE PROFILE

José Maria Esbrí
University of Castilla-La Mancha
70 PUBLICATIONS **442** CITATIONS
SEE PROFILE

Pablo León Higueras
University of Castilla-La Mancha
145 PUBLICATIONS **1,237** CITATIONS
SEE PROFILE

Manuel Valiente
Autonomous University of Barcelona
170 PUBLICATIONS **2,211** CITATIONS
SEE PROFILE

Environ. Sci. Technol. **2006**, *40,* 4090−4095

Microprobe Techniques for Speciation Analysis and Geochemical Characterization of Mine Environments: The Mercury District of Almadén in Spain

ANNA BERNAUS,[†] XAVIER GAONA,[†] JOSÉ MARIA ESBRÍ,[‡] PABLO HIGUERAS,[‡] GERALD FALKENBERG,[§] AND MANUEL VALIENTE*,[†]

Grup de Tècniques de Separació en Química (GTS), Departament de Química, Universitat Autònoma de Barcelona, 08193 Bellaterra, Barcelona, Spain, Departamento de Ingeniería Geológica y Minera, Escuela Universitaria Politécnica de Almadén, Universidad de Castilla-La Mancha, 13400 Almadén, Ciudad Real, Spain, and Hamburger Synchrotronstrahlungslabor at Deutsches Elektronen-Synchrotron DESY, Notkestrasse 85, D-22603 Hamburg, Germany

Metallurgic calcines with very high mercury and methylmercury content from the Almadén mining district were analyzed by synchrotron-based microprobe techniques. Information about mercury speciation was obtained by μ-EXAFS (microscopic extended X-ray absorption fine structure) spectroscopy, whereas elemental associations were evaluated by μ-XRF (microscopic X-ray fluorescence analysis) mapping. Complementary characterization methodologies, including X-ray diffraction (XRD), inductively coupled plasma-optical spectroscopy (ICP-OES), as well as a sequential extraction scheme (SES), were used to predict the potential availability of mercury. Analysis of total metal content revealed extremely high concentrations of mercury and iron (between 7 and 35 and 65−70 g kg^{-1}, respectively) and high zinc concentrations (2.2−2.5 g kg^{-1}), whereas other metals such as copper, nickel, and lead were found at low concentration levels (30−300 mg kg^{-1}). μ-EXAFS results indicate that cinnabar (HgS_{red}) is one of the main species within the studied mercury-rich particles (5−89% of total mercury content), together with more soluble mercury compounds such as $Hg_3(SO_4)O_2$ (schuetteite) and HgO (5−55% of total mercury content). Additionally, element-specific μ-XRF maps of selected mercury-rich particles in the studied samples revealed an evident correlation among Hg−Pb−Ni (and S), indicating a possible geochemical linkage of these elements. Correlations were also found among Fe−Mn and Hg, which have been attributed to sorption of mercury onto oxyhydroxides of Fe and Mn. This finding was supported by results from a sequential extraction scheme, where a significant amount of Hg was extracted with the fraction soluble in 6 M HCl.

Introduction

Natural mercury deposits are globally distributed in three types of mineral belts: silica−carbonate, hot-spring, and Almadén type, which are cogenetic and reflect similar tectonic and volcanic processes that contribute to the concentration of mercury (*1*). The most important of these is the Almadén mercury mineral belt in central Spain, where over one-third of the world's mercury has been produced. The mining activity dates from the Roman age, while the Hg extracted from the mine amounts to about 8.3 million Hg flasks (approximately 285 000 metric tons of Hg) (*2*). The deposit is primarily composed of cinnabar (HgS_{red}, hexagonal) and appreciable amounts of native Hg (*3*).

During metallurgical beneficiation, mercury was extracted from the mineral by volatilization, involving the crushing and roasting of the ores in large furnaces at temperatures higher than 600 °C. The process decomposes most of the Hg minerals producing Hg vapor, which is subsequently passed through condenser columns and collected as metallic (liquid) Hg in flasks. The roasted mine wastes (calcines) were typically transported short distances from the furnace and dumped in loose, unconsolidated piles, containing high Hg concentrations, typically ranging from 160 to 34 000 g kg^{-1} (*4*).

Although Hg mining activity in the Almadén district ceased in May 2002, abandoned and untreated mine wastes continue releasing Hg to the nearby streams (*5*) and the atmosphere (*6*, *7*) given the associated weathering, transport, and biological processes controlling the Hg cycle in these mine-impacted environments (*8*). Only a few studies have been conducted to evaluate the environmental impact of mercury contamination in this area (*9*−*13*). These studies show an important gap concerning the identification and quantification of inorganic mercury compounds, which are known to be the dominant components of mercury chemistry. This gap has a significant importance, because molecular-level speciation is one of the main parameters governing mercury mobility, toxicity, and bioavailability (*14*).

Recent studies have shown the applicability of synchrotron-based X-ray absorption spectroscopy (XAS) techniques to the characterization of both crystalline and noncrystalline Hg compounds in mine environments (*15*−*17*). This technique is becoming widely used for the study of molecular-level environments, showing species-specific detection capacities, while needing almost no sample pretreatment (and consequently with a minimum species modification) (*18*).

During the past decade, synchrotron-based microprobe techniques, with X-ray beams of 1−20 μm in diameter, have become increasingly utilized to map elemental distributions in environmental samples. The mapping process allows one to establish correlations among elements, while also identifying particles enriched in the target element (Hg in this study case). Both XANES (X-ray absorption near-edge structure) and EXAFS spectroscopy measurements can be performed at each spot of the incident microbeam.

The present study takes advantage of μ-XRF and μ-EXAFS microprobe techniques for the determination of mercury species in old furnace calcine samples. Complementary techniques, such as XRD, total digestion and elemental analysis by ICP-OES, or SES schemes, have been also applied to obtain an adequate knowledge of the bulk mineralogy of the sample matrixes, as well as to identify and understand

* Corresponding author phone: +34-935812903; fax: +34-935811985; e-mail: Manuel.Valiente@uab.es.
[†] Universitat Autònoma de Barcelona.
[‡] Escuela Universitaria Politécnica de Almadén.
[§] Deutsches Elektronen-Synchrotron DESY.

10.1021/es052392l CCC: $33.50

Published on Web 06/06/2006

trends within Hg association to specific matrix phases (*19*−*21*). The overall aim of this study is to utilize information on mercury speciation to predict mercury mobility and availability, as well as to relate this information to the anthropogenic and geochemical processes taking place in the Almadén environment.

Experimental Section

Sample Collection and Storage. Samples were collected at the Almadenejos decommissioned metallurgical plant, which is located some 10 km southeast of Almadén (see the Supporting Information). The plant was active during the period of the 17th to 19th century, until its closure in 1860. Two calcine samples were taken from the top of two of the old furnaces, where Gray and co-workers (*4*) quantified the highest methylmercury contents yet found in this type of samples worldwide. The two calcine samples, identified as AJ-701 and AJ-702, were collected at 10−20 cm depth using an Eijkelkamp 04.15.SA undisturbed soil sampler device, on an anthrosol (soil taxonomy, 1975) (*22*) situated on the top of the ruins of the furnace building. During sample collection, weather conditions were dry, with temperatures between 30 and 35 °C.

After collection, samples were dried and sieved to a particle size smaller than 1 cm. Then, the sieved part was milled and sieved again to <53 μm (the most suitable size for XRD and XRF analysis). Finally, and before further analyses, samples were homogenized and air-dried for 24 h. This process was considered to not modify the actual speciation of Hg in the treated samples but be most representative of the grain heterogeneity of the soil analyzed.

Mineralogical and Chemical Characterization. X-ray diffraction was used to identify the bulk mineralogy and primary matrix components of the calcines. The XRD analyses were carried out at the I. R. I. C. A. (University of Castilla-La Mancha), using a Philips diffractometer (model 1700, with Cu Kα radiation, automatic divergence aperture, and curved graphite monochromator). The reception and dispersion aperture were 0.1 mm and 1°, respectively. A Xe-filled gas was used, and the scan range was 3−75° 2Θ with a scan speed of 0.1° 2Θ s^{-1}.

Digestion of samples AJ-701 and AJ-702 was performed to quantify total metal concentration. In addition to Hg, the elemental analysis included As, Cu, Fe, Ni, Pb, Mn, and Zn. Sample digestion was carried out with an analytical microwave system (MARS-5 model from CEM Corporation, U.S.A.) and a hydrofluoric acid media, to ensure the total digestion of the sample (*23*). The electrical power steps used in the digestion process can be found elsewhere (*24*). The concentration of target elements in the aqueous solution was determined by an ICP-OES equipment (Thermo Elemental, model Iris Intrepid II XSP, U.S.A.).

Sequential Extractions. A specific SES procedure developed by the CIEMAT Research Centre (*25*) has been applied to study the distribution of Hg, As, Cu, Fe, Ni, Pb, and Mn in the calcine samples. This scheme includes six different extraction steps (*26*), which permit an accurate characterization of the heavy metal distribution among the different soil phases. The sequential extraction steps permit the identification of water-soluble compounds, exchangeable cations, carbonates fraction, easily reducible fraction, compounds soluble in 6 M HCl, and oxidizable phases. The residual metal concentration was estimated by the difference between total concentration (from HF digestion) and the sum of metal concentration within the complete extraction procedure. Detailed information on the SES experimental procedure is given as Supporting Information (see also refs *25* and *26*).

Microprobe Analyses. Microprobe analyses were performed at the synchrotron facility Hamburger Synchrotronstrahlungslabor (HASYLAB) at Deutsches Elektronen-Synchrotron DESY in Hamburg (Germany), at the bending magnet beamline L (*24*). All experiments were carried out at room temperature.

First, μ-XRF mapping was performed on samples AJ-701 and AJ-702, which provided an overview of the elemental distribution within the sample and permitted the identification of Hg-rich particles. Moreover, this mapping aims to determine spatial correlations among mercury and other elements, such as Fe and Mn, as well as other toxic elements including As, Zn, Ni, and Pb. Beamline L allows the detection of elements with atomic numbers between 13 and 92, reaching detection limits below 0.1 mg kg^{-1}, depending on the element and sample matrix. The beam was monochromatized at 13 000 eV with a Si(111) monochromator and collimated to a size of ∼15 μm diameter fwhm by using a polycapillary half-lens. The sample area around the beam position was monitored by a long-distance zoom microscope with a magnification of 300× and a CCD camera with a resolution of 3 μm. The fluorescence signal was detected with a GRESHAM Si (Li) detector and a RADIANT VORTEX silicon drift detector (50 mm^2 active area), respectively. The μ-XRF maps contained 11 × 11 points with a step size of 10 μm vertically and horizontally. The time of fluorescence signal accumulation was selected as a function of maximum total count rate of the sample and varied between 1 and 10 s per step. Elements included within the μ-XRF analysis were Hg, Fe, Mn, Ca, Cu, Ni, Pb, Ti, Zn, and S.

μ-EXAFS analyses were carried out on Hg-rich particles identified in the previous μ-XRF evaluation. For this purpose, Hg L_{III}-edge EXAFS spectra were collected from three Hg-rich particles (five replicates undertaken for each particle) identified in each calcine sample. Pure reference compounds were analyzed in transmittance mode (detection with two ionization chambers) following the Hg absorption L_{III} line at 12 284 eV. On the other hand, fluorescence detection mode was used for the analysis of unknown samples, by measuring Hg Lα1 (9988 eV) and Lα2 (9897 eV) fluorescent line intensities. Selection of the detection mode was based on sample concentration and matrix background (*27*).

Speciation data (Hg phases present and relative abundances) were obtained by comparing the spectra from the unknown samples with spectra from reference Hg minerals and pure compounds, including $HgCl_2$, Hg_2Cl_2, $HgSO_4$, HgO_{red}, $Hg(CH_3COO)_2$, CH_3HgCl, HgS_{red} (cinnabar), HgS_{black} (metacinnabar), $Hg_2NCl_{0.5}(SO_4)_{0.3}(MoO_4)_{0.1}(CO_3)_{0.1}\cdot(H_2O)$ (mosesite), $Hg_3S_2Cl_2$ (corderoite), and $Hg_3(SO_4)O_2$ (schuetteite). Reference compounds were powdered and diluted with polyethylene. Homogenization was undertaken in a vortex apparatus, and the final mixture was pressed as a pellet under 5 tons cm^{-2} for 5 min. The total amount of sample in each pellet varied from 50 to 100 mg, whereas the amount of polyethylene was kept between 100 and 150 mg.

μ-EXAFS spectra were processed by using the SixPACK data analysis software package (*28*). Spectra processing included background correction, signal normalization, and data transformation from energy to *k*-space (range considered, 1−9 $Å^{-1}$). Then, principal component analysis, PCA (*29*−*31*), was applied to derive the number and type of reference compounds from the database required to reconstruct the spectrum of an unknown sample. Finally, a linear least-squares fitting procedure was utilized to fit the spectra from the unknown samples with the spectra selected in the previous PCA analysis. The determination of the relative proportion of each reference compound contribution allows quantification of the phases present in the unknown sample. The quality of the analysis can be evaluated by the reduced chi-square value (χ^2), which represents the goodness of the model fit to the spectra data using the linear combination procedure (*32*).

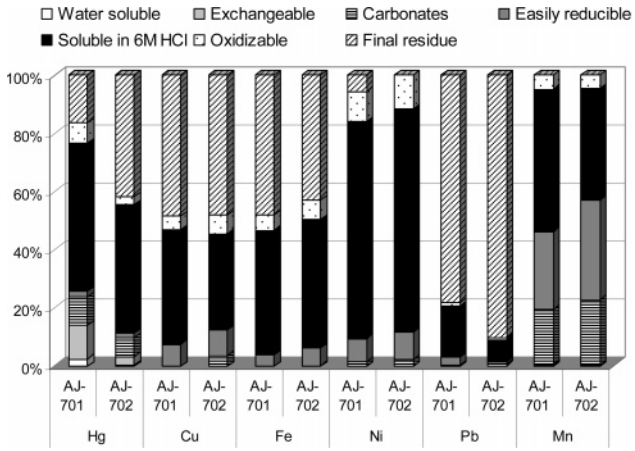

	Total content (mg kg^{-1}) AJ-701	AJ-702
Hg	35000 ± 6000	6700 ± 500
As	< 1	< 1
Cu	33 ± 7	33 ± 2
Fe	70000 ± 16000	65000 ± 2000
Ni	36 ± 6	41 ± 2
Pb	91 ± 13	276 ± 190
Mn	280 ± 60	798 ± 8
Zn	2200 ± 400	2500 ± 200

FIGURE 1. Results from the SES procedure applied to samples AJ-701 and AJ-702, and total metal content determined by HF digestion.

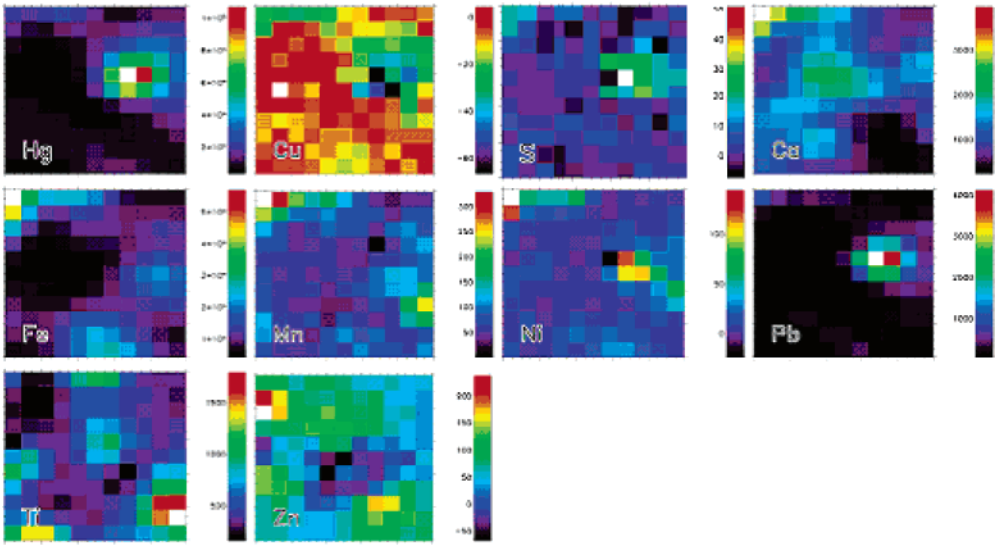

FIGURE 2. μ-XRF elemental maps for Hg, Cu, S, Ca, Fe, Mn, Ni, Pb, Ti, and Zn on a thin section (100 × 100 μm^2 area) close to particle 1 found in soil AJ-701. The color index scales indicate the measured counts s^{-1} for each element.

Results and Discussion

Mineralogical and Chemical Characterization. Results from XRD analysis highlight the predominance of phyllosilicates (mica and kaolinite, with SiO_4^{4-} partially substituted by Al^{3+} or Fe^{3+}) in both samples. This mineralogy is consistent with the geological origin of the Almadén mercury belt, because these deposits are primarily localized in Silurian quartzite adjacent to mafic craters (*1*, *2*). Plagioclase ($Na_{0.5}Ca_{0.5}Si_3AlO_8$) and calcite ($CaCO_3$) were found as typical igneous and hydrothermal minerals from the surroundings. In addition, gypsum ($CaSO_4{\cdot}2H_2O$) was detected in one of the samples (AJ-701), presumably as a product of weathering or as a building material from the furnace ruins. No Hg crystalline phases were detected by XRD, indicating their presence in relatively low proportions (below 2%).

Results of total digestion of calcine samples collected at the furnace facility of the Almadenejos mine are given in Figure 1. High mercury concentrations (compared to those of other mine facilities) have been found in these mine wastes, indicating an inefficient and incomplete Hg roasting process. This fact might also indicate the presence of unconverted cinnabar and other Hg compounds usually formed during the processing of the ore (*1*, *33*, *34*).

These results are consistent with those achieved by Gray and co-workers (*4*), where similar samples have shown mercury concentrations between 200 and 34 000 mg kg^{-1}. It is also important to note the extremely high methylmercury concentrations (between 0.2 and 3100 μg kg^{-1}) found by these authors, indicating the high methylation rates under the conditions present in this mine waste. In this sense, speciation experiments performed in our study may provide some insights about possible inorganic mercury species that underwent methylation.

Quantification of those elements that could produce spectral interferences in the XAS analysis of Hg (in fluorescence detection mode) revealed the absence of As (Kα = 10 508 eV) and relatively low concentrations of Zn (Kβ = 9572 eV) and Pb (Lα = 10 449 eV). Nevertheless, Fe (an important nonspectral interference, Kβ = 7058 eV) was found in very high concentrations, leading to a possible saturation of the fluorescence detector and consequent reduction of the detection limit of the XAS technique.

Geochemical Characterization by μ-XRF and Sequential Extraction Schemes. Figure 2 shows a set of μ-XRF elemental maps, corresponding to particle 1 from sample AJ-701. Similar results were obtained for each particle analyzed from both calcine samples. To evaluate possible correlations among elements in the samples, line intensities of all elements evaluated were extracted from each pixel in each mapping analysis. Three different correlations have been identified (see Figures 2 and 3): (i) linear Pb−Hg, Ni−Hg, and (possible) S−Hg correlations within mercury-rich areas; (ii) linear correlations among Hg and the background of Fe and Mn; (iii) no correlation among Hg and Ca, Ti, Zn, or Cu.

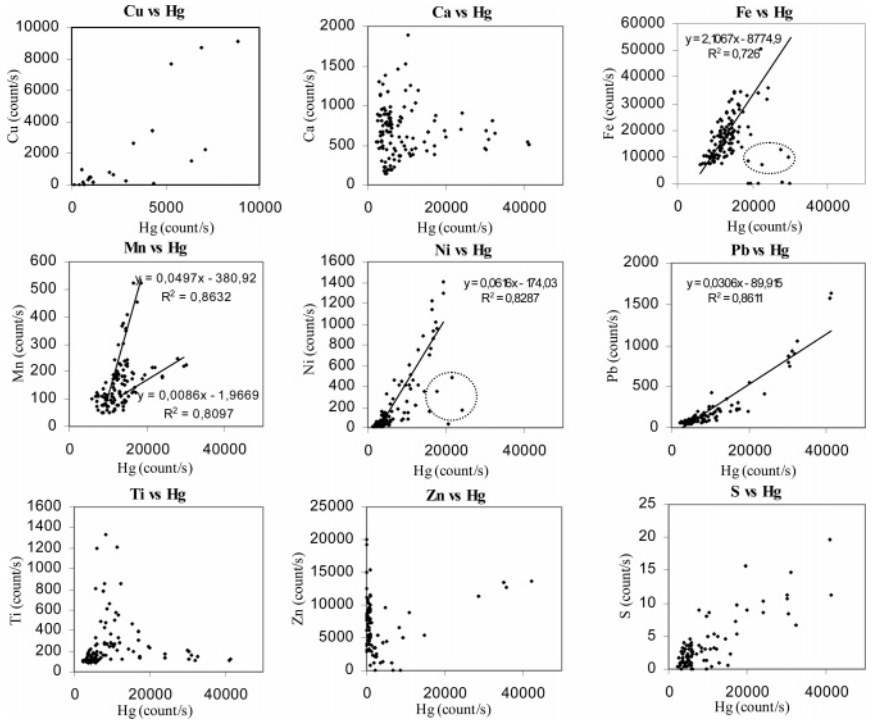

FIGURE 3. Pair correlation diagrams obtained from the μ-XRF maps of samples AJ-701 and AJ-702 (average of six regions belonging to the mercury-rich particles), as fluorescence line intensity (counts s^{-1}). Outliers of Fe and Ni (dashed circles) are not considered for linear regressions.

The observed association trend among Hg−Pb−Ni might be explained by the well-known tendency of these three elements to form very stable compounds with sulfide. In this sense, Figure 3 might also corroborate the affinity of Hg toward S, taking into account that sulfur is a "soft" Lewis base that can form strong covalent bonds with the highly polarizable mercury atom ("soft" Lewis acid). However, the correlation Hg−S must be taken with care, given the low count rate shown by S. Further interpretations of the Hg−Pb−Ni−S correlation are driven by SES analyses (see below).

Figure 3 points out significant Fe−Hg and Mn−Hg correlations. In both cases, the main correlation is found within the sample background, instead of the mercury-rich particles. The correlation Fe−Hg might be explained by two hypotheses: (i) there may be phase association between cinnabar and pyrite. Nevertheless, this option has been disregarded given the low presence of pyrite in the area. (ii) There may be sorption of mercury onto Fe oxyhydroxides. According to Kim and co-workers (*16*), Hg(II) sorbs strongly to fine-grained powders of goethite (α-FeOOH) with a sorption density of 0.39−0.42 μmol m^{-2}. Iron oxyhydroxides are also known as effective substrates for Hg sorption in natural aquatic systems, where Hg(II) forms bidentate inner-sphere complexes with the substrate surface (*16*, *35*).

Hg(II) is also known to form inner-sphere complexes with manganese oxides (*1*). Although Mn is found in lower concentration than Fe in the Almadén mine wastes (see Table 1), this fact might explain the linear correlation observed between Hg and Mn. In this sense, Figure 3 shows two different tendencies concerning the Hg−Mn linear correlation, which may indicate the occurrence of two different sorption processes.

To corroborate the presence of Hg sorbed onto oxyhydroxides of Fe and Mn, the SES procedure developed by CIEMAT was applied to samples AJ-701 and AJ-702. This procedure also provides useful information on the potential mobilization of mercury (*25*, *36*).

Results of the SES procedure applied to samples AJ-701 and AJ-702 (Figure 1) indicate that the mercury distribution in both samples is relatively similar. Mercury extracted with 6 M HCl (51% AJ-701, 44% AJ-702) has been found to be exceptionally high compared with other steps, which can be explained by the strong binding of Hg(II) to crystalline Fe−Mn oxyhydroxides or sulfides. On the other hand, the easily reducible fraction releases little mercury (4% in both samples), suggesting the lack of Hg associated with amorphous Fe−Mn oxyhydroxides or to organic matter. Concerning the average Hg concentrations found in the final residue (16% AJ-701, 42% AJ-702), these would correspond to HgS (either cinnabar or metacinnabar). Finally, the significant mercury concentrations found in the water-soluble, exchangeable, and carbonate fractions are related to the presence of more soluble mercury compounds, therefore posing an evident risk of mercury mobilization. This fact has been also ascertained by the following μ-EXAFS analyses.

TABLE 1. Chemical Speciation of Hg-Rich Particles from Calcine Samples of the Almadenejos Mercury Mine[a]

sample	cinnabar	HgO	schuetteite	χ^2
AJ-701; particle 1	< 5	47	49	0.17
AJ-701; particle 2	34	41	24	0.74
AJ-701; particle 3	9	55	36	0.26
AJ-702; particle 1	89	5	6	0.23
AJ-702; particle 2	26	47	27	1.68
AJ-702; particle 3	14	38	47	1.32

[a] Concentration values expressed in percent relative to the total mercury content in each sample.

Concerning other metal components, nickel is principally found in the fifth extraction step, therefore being associated to crystalline Fe−Mn oxyhydroxides. On the other hand, lead is not extracted but mainly remains in the final residue (see Figure 1), thus providing similar behavior as Hg that is expected to be found as a sulfide compound. This information helps to understand the Hg−Pb and Hg−Ni correlations found by μ-XRF. Thus, mixed Hg−Pb−S compounds are expected to be present in the samples analyzed, while Hg

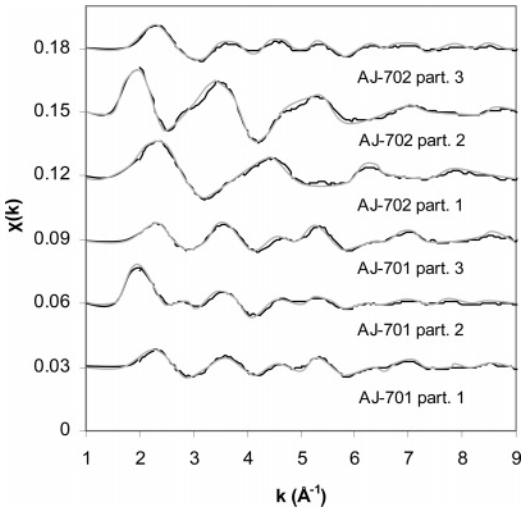

FIGURE 4. Linear combination fits of the samples (black line = raw data, gray line = fit). (Note the deliberate offset of spectra to show differences.) Each spectrum is the mean value of five replicates.

and Ni correlations might be explained by the related sorption of these metals on crystalline Fe−Mn oxyhydroxides.

Speciation Analysis by μ-EXAFS. Results of PCA using the L_{III}-edge EXAFS spectra from Hg-rich particles found in the calcine samples indicate that a minimum of four components (cinnabar, HgO, schuetteite, and $HgCl_2$) are required to reconstruct each of the experimental spectra above the 95% confidence level. As stated in the Experimental Section, the original set of reference compounds included 11 mercury phases.

On the basis of the previous PCA analysis, Figure 4 shows the corrected EXAFS spectra for all the particles evaluated from samples AJ-701 and AJ-702, as well as the spectra obtained by linear combination of the four reference compounds, determined by the fitting procedure. The relative proportions of each reference compound identified in each μ-EXAFS analysis, as well as the reduced chi-square value (χ^2) associated with the related fit, are given in Table 1.

A diversity of speciation results from mercury-rich particles has been obtained in both samples, indicating the significant heterogeneity of the samples. Cinnabar is present in most of the particles (5−89% of the total mercury content), although schuetteite and HgO (both more soluble than cinnabar) have also been identified in high proportions (5−55% of the total mercury content). This fact results in a significant source of relatively mobile mercury. Indications of the possible presence of $HgCl_2$ have been observed within the fitting procedure, although in nonsignificant proportions.

These speciation results are not consistent with those previously published (*17*, *24*) dealing with Almadén calcine samples, where significant concentrations of metacinnabar were identified by EXAFS. The presence of this metastable polymorph of cinnabar is consistent with the high temperatures applied to the mineral during the extraction process.

The historical investigation of the Almadenejos mine and its furnace facilities brought to light the high Hg losses through the oven ashtrays, piping, and chimneys, as well as the very low efficiency of the roasting procedure applied at this facility (*37*). As a result of the lower ore roasting temperatures, lower mercury recovery was achieved (see the extremely high mercury concentrations, Figure 1). This finding helps to explain the lower conversion of cinnabar to metacinnabar found in our studies of the site.

The presence of schuetteite (and probably of $HgCl_2$) is related to supergene alteration of cinnabar, as shown by the common presence of schuetteite in many mine dumps, especially on sunlight-exposed rocks (*11*).

As stated before, previous studies undertaken by Gray and co-workers (*4*) showed the extremely high methylmercury concentrations present within the analyzed calcine samples, compared with those of similar samples from other mine and metallurgic facilities worldwide. Therefore, the identification of the inorganic source species for the biomethylation processes becomes of a significant importance for the overall definition of the mercury cycle. In this context, this study shall be considered as a first approach to understand the insights of this process.

Summarizing, the proposed coupling of techniques have demonstrated the existence of relatively soluble Hg phases in the analyzed calcine samples, which might be mobilized through different weathering processes. This fact poses an evident risk both to the biota and to human beings, given the well-known mercury toxicity. Nevertheless, it must be highlighted that these conclusions are driven in the frame of a reduced number of samples, and therefore, the analysis of additional samples could contribute positively to the robustness of such indication.

The presented coupling of techniques may be considered as a good alternative to the more traditional solid-phase speciation based on chemical information and, therefore, a useful tool to consider when assessing the risk associated to mobility and potential bioavailability of Hg.

Acknowledgments

Synchrotron experiments at HASYLAB were financially supported by the European Community−Research Infrastructure Action under the FP6 "Structuring the European Research Area" Program (through the Integrated Infrastructure Initiative "Integrating Activity on Synchrotron and Free Electron Laser Science"). Anna Bernaus thanks the Ministry of Science and Education for a Ph.D. scholarship (2003−2005). The Spanish Project PPQ2002-04267-C03-01 provided financial support for the present study. Projects PPQ2003-01902 and PCC-05-004-3 also contributed to related expenses. Gordon Brown (Stanford University) is thanked for helpful comments on the manuscript after it was submitted to ES&T for review.

Supporting Information Available

Figure detailing the location of the mines, metallurgical plants, and the sampling area and a table outlining the sequential extraction procedure. This material is available free of charge via the Internet at http://pubs.acs.org.

Literature Cited

(1) Rytuba, J. J. Mercury from mineral deposits and potential environmental impacts. *Environ. Geol.* **2003**, *43*, 326−338.

(2) Hernández, A.; Jébrak, M.; Higueras, P.; Oyarzun, R.; Morata, D.; Munhá, J. The Almadén mercury mining district, Spain. *Mineralium Deposita* **1999**, *34*, 539−548.

(3) Rytuba, J. J.; Rye, R. O.; Hernandez, A. M.; Dean, J. A.; Arribas, A. Characterisation of Almadén mercury mine environment by XAS techniques. *Int. Geol. Congr. Abstr. Prog.* **1988**, 2−741.

(4) Gray, J. E.; Hines, M. E.; Higueras, P. L.; Adatto, I.; Lasorsa, B. K. Mercury speciation and microbial transformations in mine wastes, stream sediments, and surface waters at the Almadén Mining District, Spain. *Environ. Sci. Technol.* **2004**, *38*, 4285−4292.

(5) Ganguli, P. M.; Mason, R. P.; Abu-Saba, K. E.; Anderson, R. S.; Flegal, A. R. Fishing for identity: mercury contamination and fish consumption among indigenous groups in the United States. *Sci., Technol. Soc.* **2000**, *34* (22), 4773−4779.

(6) Gustin, M. S.; Coolbaugh, M.; Engle, M.; Fitzgerald, B.; Keislar, R.; Lindberg, S. E.; Nacht, D.; Quashnick, J.; Rytuba, J.; Sladek, C.; Zhang, H.; Zehner, R. Atmospheric mercury emissions from mine wastes and surrounding geologically enriched terrains. *Environ. Geol.* **2003**, *43*, 339−351.

(7) Gustin, M. S.; Lindberg, S. E.; Austin, K.; Coolbaugh, M.; Vette, A.; Zhang, H. Assessing the contribution of natural sources to

regional atmospheric mercury budgets. *Sci. Total Environ.* **2000**, *259* (1−3), 61−71.
(8) Wershaw, R. L. Sources and behaviour of mercury in surface waters; Mercury in the Environment. *U.S. Geol. Surv Prof. Pap.* **1970**, *713*, 29−34.
(9) Berzas Nevado, J. J.; García Bermejo, L. F.; Rodríguez Martín-Doimeadios, R. C. Distribution of mercury in the aquatic environment at Almadén, Spain. *Environ. Pollut.* **2003**, *122*, 261−271.
(10) Ferrara, R.; Maserti, B. E.; Andersson, M.; Edner, H.; Ragnarson, P.; Svanberg, S.; Hernandez, A. Atmospheric mercury concentrations and fluxes in the Almadén district (Spain). *Atmos. Environ.* **1998**, *32*, 3897−3904.
(11) Higueras, P.; Oyarzun, R.; Biester, H.; Lillo, J.; Lorenzo, S. J. A first insight into mercury distribution and speciation in soils from the Almadén mining district, Spain. *Geochem. Explor.* **2003**, *80*, 95−104.
(12) Higueras, P.; Oyarzun, R.; Lillo, J.; Sánchez Hernández, J. C.; Molina, J. A.; Esbrí, J. M.; Lorenzo, S. The Almadén district (Spain): anatomy of one of the world's largest Hg-contaminated sites. *Sci. Total Environ.* **2005**, *356*, 112−124.
(13) Moreno, T.; Higueras, P.; Jones, T.; McDonald, I.; Gibbons, W. Size fractionation in mercury-bearing airborne particles (HgPM10) at Almadén, Spain: implications for inhalation hazards around old mines. *Atmos. Environ.* **2005**, *39*, 6409−6419.
(14) Brown, G. E., Jr.; Foster, A. L.; Ostergren, J. D. Mineral surfaces and bioavailability of heavy metals: a molecular-scale perspective. *Proc. Natl. Acad. Sci. U.S.A.* **1999**, *96*, 3388−3395.
(15) Kim, C. S.; Rytuba, J. J.; Brown, G. E., Jr. Geological and anthropogenic factors influencing mercury speciation in mine wastes: an EXAFS spectroscopy study. *Appl. Geochem.* **2004**, *19* (3), 379−393.
(16) Kim, C. S.; Rytuba, J. J.; Brown, G. E., Jr. EXAFS study of Hg(II) sorption to Fe- and Al-(hydr)oxide surfaces: I. Effects of pH. *J. Colloid Interface Sci.* **2004**, *271* (1), 1−15.
(17) Kim, C. S.; Brown, G. E., Jr.; Rytuba, J. J. Characterization and speciation of mercury-bearing mine wastes using X-ray absorption spectroscopy (XAS). *Sci. Total Environ.* **2000**, *261* (1−3), 157−168.
(18) Morin, G.; Juillot, F.; Ostergren, J. D.; Ildefonse, P.; Calas, G.; Brown, G. E., Jr. XAFS determination of the chemical form of lead in smelter-contaminated soils and mine tailings: importance of adsorption processes. *Am. Mineral.* **1999**, *84*, 420−434.
(19) Quevauviller, P. Operationally defined extraction procedures for soil and sediments analysis I. Standardization. *TrAC, Trends Anal. Chem.* **1998**, *17*, 89−298.
(20) Davidson, C. M. M.; Duncan, A. L.; Littlejohn, D.; Ure, A. M.; Garden, L. M. A critical evaluation of the three-stage BCR sequential extraction procedure to assess the potential mobility and toxicity of heavy metals in industrially contaminated land. *Anal. Chim. Acta* **1998**, *363*, 45−55.
(21) Fedotov, P. S.; Zavarzina, A. G.; Spivakov, B. Y.; Wennrich, R.; Mattusch, J.; de Cunhal-Titze, K. P.; Demin, V. V. Accelerated fractionation of heavy metals in contaminated soils and sediments using rotating coiled columns. *J. Environ. Monit.* **2002**, *4*, 318−324.
(22) Soil Survey Staff. *Soil Taxonomy: A Basic System of Soil Classification for Making and Interpreting Soil Surveys*; U.S. Department of Agriculture Handbook No. 436; U.S. Department Agriculture: Washington, DC, 1975.
(23) Fernández-Martínez, R.; Rucandio, M. I. Study of extraction conditions for the quantitative determination of Hg bound to sulfide in soils from Almadén (Spain). *Anal. Bioanal. Chem.* **2003**, *375*, 1089−1096.
(24) Bernaus, A.; Gaona, X.; Valiente, M. Characterisation of Almadén mercury mine environment by XAS techniques. *J. Environ. Monit.* **2005**, *7*, 771−777.
(25) Pérez del Villar, L.; Quejido, A. J.; Crespo, M. T.; Sánchez, M.; Cózar, J. S.; Galán, M. P.; Fernández-Díaz, M. Sequential leaching methods: review, previous experiences and proposed method for Fe(III)−U(VI)-rich fracture filling materials. *Trends Geochem.* **2002**, *2*, 19−42.
(26) Sánchez, D. M.; Quejido, A. J.; Fernández, M.; Hernández, C.; Schmid, T.; Millán, R.; González, M.; Aldea, M.; Martín, R.; Morante, R. Mercury and trace element fractionation in Almadén soils by application of different sequential extraction procedures. *Anal. Bioanal. Chem.* **2005**, *381*, 1507−1513.
(27) Waychunas, G. A.; Brown, G. E., Jr. Fluorescence yield XANES and EXAFS experiments: application to highly dilute and surface samples. *Adv. X-Ray Anal.* **1994**, *37*, 607−617.
(28) Webb, S. M. SIXPack: a graphical user interface for XAS analysis using IFEFFIT. *Phys. Scr.* **2005**, *T115*, 1011−1014.
(29) Malinowski, E. R. *Factor Analysis in Chemistry*, 2nd ed.; Wiley & Sons: New York, 1991; p 350.
(30) Ressler, T.; Wong, J.; Roos, J.; Smith, I. L. Quantitative speciation of Mn-bearing particulates emitted from autos burning (methylcyclopentadienyl)manganese tricarbonyl-added gasolines using XANES spectroscopy. *Environ. Sci. Technol.* **2000**, *34* (6), 950−958.
(31) Wasserman, S. R.; Allen, P. G.; Shuh, D. K.; Bucher, J. J.; Edelstein, N. M. EXAFS and principal component analysis: a new shell game. *J. Synchrotron Radiat.* **1999**, *6*, 284−286.
(32) Slowey, A. J.; Johnson, S. B.; Rytuba, J. J.; Brown, G. E., Jr. Role of organic acids in promoting colloidal transport of mercury from mine tailings. *Environ. Sci. Technol.* **2005**, *39* (20), 7869−7874.
(33) Kim, C. S.; Rytuba, J. J.; Bloom, N. S.; Brown, G. E., Jr. Mercury speciation by X-ray absorption fine structure (XAFS) spectroscopy and sequential chemical extractions: a comparison study. *Environ. Sci. Technol.* **2003**, *37*, 5102−5108.
(34) Biester, H.; Gosar, M.; Müller, G. Mercury speciation in tailings of the Idrija mercury mine. *J. Geochem. Explor.* **1999**, *65*, 195−204.
(35) Collins, C. R.; Sherman, D. M.; Ragnarsdottir, K. V. Surface complexation of Hg^{2+} on goethite: mechanism from EXAFS spectroscopy and density functional calculations. *J. Colloid Interface Sci.* **1999**, *219*, 345−350.
(36) Davidson, C. M.; Thomas, R. P.; McVey, S. E.; Perala, R.; Littlejohn, D.; Ure, A. U. Evaluation of sequential extraction procedure for speciation of heavy metals in sediments. *Anal. Chim. Acta* **1994**, *291*, 277−286.
(37) Sumozas, R. Arquitectura Industrial en Almadén: Antecedentes, Génesis y Extensión de un Modelo, Ph.D. Thesis, University of Castilla−La Mancha, 2005; pp 171−202.

Received for review November 29, 2005. Revised manuscript received April 20, 2006. Accepted May 4, 2006.

ES052392L